



**HAL**  
open science

## Hydrogenation of solid hydrogen cyanide HCN and methanimine CH<sub>2</sub>NH at low temperature

Patrice Theulé, Fabien Borget, Florent Mispelaer, Grégoire Danger, Fabrice Duvernay, Jean-Claude Guillemin, Thierry Chiavassa

► **To cite this version:**

Patrice Theulé, Fabien Borget, Florent Mispelaer, Grégoire Danger, Fabrice Duvernay, et al.. Hydrogenation of solid hydrogen cyanide HCN and methanimine CH<sub>2</sub>NH at low temperature. *Astronomy and Astrophysics - A&A*, 2011, 534, pp.A64. 10.1051/0004-6361/201117494 . hal-00844618

**HAL Id: hal-00844618**

**<https://hal.science/hal-00844618>**

Submitted on 20 Aug 2013

**HAL** is a multi-disciplinary open access archive for the deposit and dissemination of scientific research documents, whether they are published or not. The documents may come from teaching and research institutions in France or abroad, or from public or private research centers.

L'archive ouverte pluridisciplinaire **HAL**, est destinée au dépôt et à la diffusion de documents scientifiques de niveau recherche, publiés ou non, émanant des établissements d'enseignement et de recherche français ou étrangers, des laboratoires publics ou privés.

# Hydrogenation of solid hydrogen cyanide HCN and methanimine CH<sub>2</sub>NH at low temperature

P. Theule<sup>1</sup>, F. Borget<sup>1</sup>, F. Mispelaer<sup>1</sup>, G. Danger<sup>1</sup>, F. Duvernay<sup>1</sup>, J. C. Guillemin<sup>2</sup>, and T. Chiavassa<sup>1</sup>

<sup>1</sup> Université de Provence, Laboratoire de Physique des Interactions Ioniques et Moléculaires, Centre de St-Jérôme, Avenue Escadrille Normandie-Niémén, 13397 Marseille, France  
e-mail: patrice.theule@univ-provence.fr

<sup>2</sup> Sciences Chimiques de Rennes, École Nationale Supérieure de Chimie de Rennes, CNRS, UMR 6226, Avenue du Général Leclerc, CS 50837, 35708 Rennes Cedex 7, France

Received 16 June 2011 / Accepted 7 August 2011

## ABSTRACT

**Context.** Hydrogenation reactions dominate grain surface chemistry in dense molecular clouds and lead to the formation of complex saturated molecules in the interstellar medium.

**Aims.** We investigate in the laboratory the hydrogenation reaction network of hydrogen cyanide HCN.

**Methods.** Pure hydrogen cyanide HCN and methanimine CH<sub>2</sub>NH ices are bombarded at room temperature by H-atoms in an ultra-high vacuum experiment. Warm H-atoms are generated in an H<sub>2</sub> plasma source. The ices are monitored with Fourier-transform infrared spectroscopy in reflection absorption mode. The hydrogenation products are detected in the gas phase by mass spectroscopy during temperature-programmed desorption experiments.

**Results.** HCN hydrogenation leads to the formation of methylamine CH<sub>3</sub>NH<sub>2</sub>, and CH<sub>2</sub>NH hydrogenation leads to the formation of methylamine CH<sub>3</sub>NH<sub>2</sub>, suggesting that CH<sub>2</sub>NH can be a hydrogenation-intermediate species between HCN and CH<sub>3</sub>NH<sub>2</sub>.

**Conclusions.** In cold environments the HCN hydrogenation reaction can produce CH<sub>3</sub>NH<sub>2</sub>, which is known to be a glycine precursor, and to destroy solid-state HCN, preventing its observation in molecular clouds ices.

**Key words.** astrochemistry – ISM: molecules – molecular processes

## 1. Introduction

Surface hydrogenation reactions play an important role in the evolution of molecules on interstellar ices, especially at low temperatures in dense molecular clouds where the secondary photon field is very weak and where hydrogen atoms have an important residence time on the surface. Very few studies have been carried out on these hydrogenation reactions. Hiraoka et al. (1994), Watanabe et al. (2002), and Fuchs et al. (2009) show how H<sub>2</sub>CO and CH<sub>3</sub>OH can be formed from the hydrogenation of CO. The solid-state H<sub>2</sub>O formation routes from the hydrogenation of the oxygen atom (Hiraoka et al. 1998; Dulieu et al. 2010), from the dioxygen molecule (Miyachi et al. 2008; Ioppolo et al. 2008; Matar et al. 2008) and from the ozone molecule (Mokrane et al. 2009; Romanzin et al. 2011) have been extensively studied. The formation of C<sub>2</sub>H<sub>5</sub>OH, CH<sub>3</sub>OH, H<sub>2</sub>CO and CH<sub>4</sub> from the hydrogenation of CH<sub>3</sub>CHO has also been studied by (Bisschop et al. 2007), as well as the formation of HCOOH from the hydrogenation of a CO:O<sub>2</sub> mixture (Ioppolo et al. 2011). It is important to have a detailed reaction network of these hydrogenation processes because they have reaction rates faster than thermal or photochemical reactions at low temperatures and under a weak radiation field. In addition, the residence time of the hydrogen atoms on ice surface makes these reactions dominant in grain surface chemistry at low temperature. Moreover, HCN is a key molecule in interstellar chemistry because it is the simplest molecule containing a CN moiety, which is a prerequisite to form amino-acids (Ferris et al. 1984).

We bombarded solid hydrogen cyanide HCN and methanimine CH<sub>2</sub>NH with warm H-atoms generated from an H<sub>2</sub> plasma source to obtain the hydrogenation reaction network of HCN at low temperature. We used Fourier-transform reflection absorption infrared spectroscopy (RAIRS) to monitor the ice analog composition, and mass spectrometry to detect the hydrogenation products during temperature-programmed desorption experiments. We show that HCN can be hydrogenated into fully saturated methylamine CH<sub>3</sub>NH<sub>2</sub>, and that methanimine CH<sub>2</sub>NH can also be hydrogenated into CH<sub>3</sub>NH<sub>2</sub>. It has been shown that methylamine CH<sub>3</sub>NH<sub>2</sub> can thermally react with CO<sub>2</sub> in the solid phase to form a carbamate, which can be converted in a glycine salt under VUV irradiation. This glycine salt eventually thermally desorbs as gas-phase-neutral glycine NH<sub>2</sub>CH<sub>2</sub>COOH (Bossa et al. 2009).

## 2. Experimental

The experiments were performed using our RING experimental set-up as described elsewhere (Theule et al. 2011). A polished copper surface is maintained at 15 K using a closed-cycle helium cryostat (ARS Cryo, model DE-204 SB, 4 K cryogenerator) within a high-vacuum chamber at a few 10<sup>-9</sup> mbar. Ice analogs are formed by spraying a room-temperature gas onto the polished copper surface. The infrared spectra are recorded by means of Fourier-transform reflection absorption infrared Spectroscopy (FT-RAIRS) using a Vertex 70 spectrometer with a MCT detector. A typical spectrum has a 1 cm<sup>-1</sup> resolution and is averaged

over a few hundred interferograms. Final hydrogenation products are detected in the gas phase after thermal desorption from the substrate, which is warmed using a heating resistance. The sample temperature is measured with a DTGS 670 Silicon diode with a 0.1 K uncertainty, and controlled using a Lakeshore Model 336 temperature controller. Gas-phase species are detected by means of mass spectrometry, using a Hiden HAL VII RGA quadrupole mass spectrometer. The ionization source is a 70 eV impact electronic source and the mass spectra are recorded between 1 and 60 amu. In a typical temperature-programmed desorption experiment (TPD), the mass spectra are recorded as the products are being desorbed during a 5 K/min temperature ramp.

Warm atomic hydrogen is produced from a molecular hydrogen plasma source. The plasma is generated from a 2.45 GHz microwave discharge (Ophos Instruments Inc.) within an Evenson cavity (Fehsenfeld et al. 1965) where molecular hydrogen gas is flowing in a 13 mm diameter pyrex tube at approximately  $5 \times 10^{-2}$  mbar. A few microns diameter 5 mm long pyrex capillary allows one to extract hydrogen atoms from the plasma. Charged particles ( $H^+$ ,  $H_2^+$ ,  $e^-$ , ...) recombine quickly within the capillary because of its small diameter. However, we do not know the cation-electron recombination rate within the capillary and thus the overall hydrogen atom yield at the capillary output. At the output of the capillary, a 13 mm diameter pyrex elbow tube prevents photons generated in the plasma from reaching the ice-analog sample. Because the mean free path of the hydrogen atoms is much smaller than the dimensions of the elbow tube, hydrogen atoms undergo several collisions in the room-temperature tube, which means that the kinetic energy of the warm hydrogen atoms impinging on the ice analog sample must be around 300 K. We calibrated the atomic hydrogen flux by hydrogenating CO following Watanabe et al. (2002). A CO ice at 15 K is exposed to the hydrogen beam and the  $H_2CO$  band at  $1720\text{ cm}^{-1}$  is monitored along with time using FTIR spectroscopy. In our experimental conditions, the formed quantity of  $H_2CO$  reaches the plateau after approximately 150–200 min of exposure. Following Watanabe et al. (2002), we can make a rough estimate of our H flux to few  $10^{14}\text{ cm}^{-2}\text{ s}^{-1}$ . The tube is directly connected to the high-vacuum chamber, facing the sample holder, so that the pressure within the chamber is a few  $10^{-6}$  mbar when a  $5 \times 10^{-2}$  mbar molecular hydrogen pressure is at the input of the capillary tube. A 15 K temperature is chosen during the hydrogenation experiments to prevent condensation of  $H_2$  on the surface. We chose a sufficiently low temperature to allow the hydrogen atoms to remain long on the surface but the temperature was initially high enough to allow hydrogen atoms to have a high mobility to move on the surface and penetrate as deep as possible into the bulk of the ice, and also to overcome a possible activation barrier at hydrogenation, if a Langmuir-Hinshelwood mechanism were present. A typical hydrogenation experiment lasts around three hours, which corresponds to a dose of  $10^{18}\text{ cm}^{-2}$  of warm H-atoms.

The HCN monomer is synthesized from the thermal reaction of potassium cyanide KCN and an excess of stearic acid  $CH_3(CH_2)_{16}COOH$  in a primary pumped vacuum line, as described in Gerakiness et al. (2004). The methanimine  $CH_2NH$  monomer was obtained from the dehydrocyanation of aminoacetonitrile following the synthesis protocol described in Guillemin and Denis (1988). Briefly, in a first step, aminoacetonitrile  $NH_2CH_2CN$  is synthesized from aminoacetonitrile hydrogensulfate  $NCCH_2NH_3^+HSO_4^-$  in powder suspended in dichloromethane  $CH_2Cl_2$ , by bubbling ammonia in the solution to neutralize the acid. Then, aminoacetonitrile is thermolyzed at

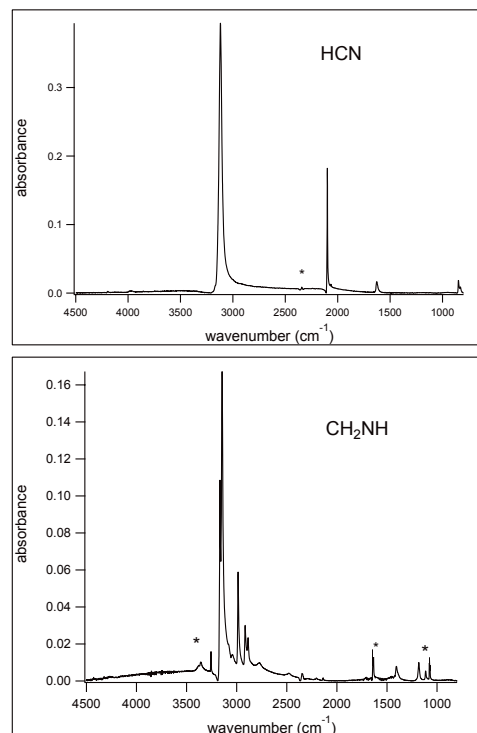


**Fig. 1.** Pure hydrogen cyanide HCN (*top*) and methanimine  $CH_2NH$  (*bottom*) infrared spectrum at  $T = 15\text{ K}$  before hydrogenation. Synthesis by-products are observed from their bands marked with an asterisk. The bands at  $1010$ ,  $1628$ , and  $3377\text{ cm}^{-1}$  correspond to  $NH_3$  remaining from the  $CH_2NH$  synthesis, and the band at  $2349\text{ cm}^{-1}$  corresponds to  $CO_2$  issued from the decomposition of stearic acid during the HCN synthesis.

$600\text{ }^\circ\text{C}$  to form methanimine and hydrogen cyanide. The latter is selectively trapped on KOH and the methanimine monomer is trapped in liquid nitrogen. Methanimine is a kinetically unstable compound that can be kept few hours in dry ice but indefinitely in liquid nitrogen.

### 3. Results

#### 3.1. Hydrogenation of pure hydrogen cyanide HCN

Gas-phase HCN is sprayed onto the polished copper surface maintained at 15 K. After deposition, the purity of the sample is checked on an IR spectrum, as seen in Fig. 1. Very little  $CO_2$  impurity originating from the HCN synthesis is present in the spectra. The IR bands of the different species are listed in Table 1 along with their corresponding assignments.

Solid HCN is exposed to the warm atomic hydrogen beam at 15 K during a fixed amount of time. Three hydrogenation experiments are performed during 20 min, one hour, and three hours, respectively. The three-hours experiment was repeated several times to check for the reproducibility. A reference experiment was performed where  $H_2$  was kept a long time at 15 K without being exposed to the hydrogen beam. We do not observe hydrogenation products in the IR spectra after hydrogenation, owing to a low hydrogenation yield. To detect the hydrogenation products the sample is warmed to room-temperature during a TPD experiment. Temperature-programmed desorption mass spectra are recorded for HCN samples that are exposed to H atoms and those that are not. These spectra are normalized to take into account that slightly different quantities of HCN are deposited

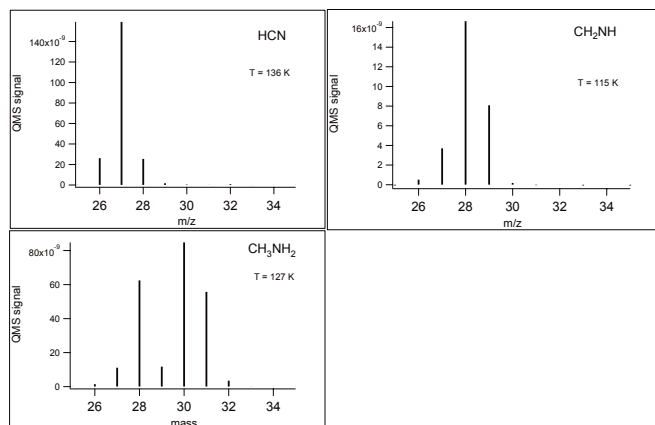


**Fig. 2.** Bar mass spectra of hydrogen cyanide HCN, methanimine CH<sub>2</sub>NH, and methylamine CH<sub>3</sub>NH<sub>2</sub> at  $T = 114$  K,  $T = 115$  K and  $T = 126$  K respectively.

**Table 1.** Fundamental infrared band positions (cm<sup>-1</sup>), with their assignments of HCN, CH<sub>2</sub>NH and CH<sub>2</sub>NH<sub>3</sub> at 10 K.

Vibration mode	HCN <sup>a</sup>	CH <sub>2</sub> NH <sup>b</sup>	CH <sub>3</sub> NH <sub>2</sub> <sup>c</sup>
N-H <sub>as</sub> stretch			3343
N-H <sub>s</sub> stretch			3282
N-H stretch		3266	
C-H stretch	3118		
C-H <sub>as</sub> stretch		3162/3140	2967/2942/2920
C-H <sub>s</sub> stretch		2987/2916/2886	2897/2883/2862
C≡N stretch	2099		
C=N stretch		1642/1634	
NCH bend overtone	1628		
NH <sub>2</sub> bend			1615
CH <sub>3as</sub> bend			1478/1455
CH <sub>3s</sub> bend			1420
CH <sub>2</sub> scissoring		1411	
NH <sub>2</sub> torsion		1186	1339
CH <sub>3</sub> rocking			1156
NH torsion		1117	
C-N stretch			1042
NH <sub>2</sub> wagging			997/896
NCH bending	849		

**References.** <sup>(a)</sup> Gerakines et al. (2004); <sup>(b)</sup> Hamada et al. (1984); Jacox et al. (1975); <sup>(c)</sup> Bossa et al. (2008).

from one experiment to another. For each experiment the HCN<sup>+</sup> molecular ion  $m/z$  27 peak, which is not sensitive to any possible N<sub>2</sub> pollution, is integrated and the spectra of all masses are scaled by dividing them by the integration result. In this way can compare mass spectra originating from different experiments.

Figure 2 shows the relative intensities of the different masses in hydrogen cyanide HCN, methanimine CH<sub>2</sub>NH, and methylamine CH<sub>3</sub>NH<sub>2</sub> mass spectra for reference. HCN has a strong peak at  $m/z$  27, CH<sub>2</sub>NH has two strong peaks at  $m/z$  28 and 29 and CH<sub>3</sub>NH<sub>2</sub> has two strong peaks at  $m/z$  30 and 31.

First Fig. 3 shows that there is a big change in the ice morphology. A TPD spectrum of bulk HCN, without H atoms bombardment, shows a clear zeroth-order desorption curve. However, when exposed to the hydrogen beam, the zeroth-order desorption curve is altered and shifted to higher temperature, and this change is function of the exposure time.

We can derive the amount of deposited HCN from IR spectra after deposition and prior H atoms bombardment by integrating the CN stretching band at 2099 cm<sup>-1</sup>. A band strength of

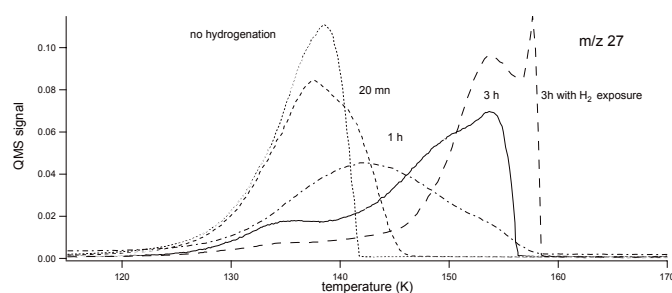


**Fig. 3.** Temperature-programmed desorption curves of  $m/z$  27 of hydrogen cyanide HCN without exposure to the room-temperature atomic H-beam at 15 K (dotted line), and with exposure during 20 min (dashed line), one hour (dotted-dashed line) and three hours (full line). The warm atomic H<sub>2</sub> beam induces a change in morphology that shifts the desorption maximum to higher temperatures, as shown by the TPD curve obtained after three hours exposure to the H<sub>2</sub> beam with the plasma discharge off (large dashed line).

$5.1 \times 10^{18}$  cm molecule<sup>-1</sup> is taken for this band (Gerakines et al. 2004). The ratio between the TPD spectrum  $m/z$  27 integral and the IR spectrum at 2099 cm<sup>-1</sup> band integral is the same for the unexposed sample and the different exposed samples. This means that the whole  $m/z$  band belongs to HCN and that the changes in the desorption curve do not correspond to the fragmentation of other heavier species. It also means that the hydrogenation yield is small, which explains that we cannot observe any hydrogenation products using IR spectroscopy. Therefore we conclude that the modified desorption curve of HCN is instead caused by a change in morphology than by a conversion in more saturated species.

This change in morphology of ice analogs after hydrogen atom exposure has already been shown (Accolla et al. 2010). Control experiments where the HCN ice is i. deposited at 15 K and kept at 15 K for three hours ii. deposited at 100 K iii. deposited at 15 K and then annealed at 100 K, give roughly similar TPD curves as the unexposed HCN ice. However, if the HCN ice is exposed to a pure H<sub>2</sub> beam (plasma discharge off) at 15 K for three hours, its TPD curve is similar to that of the HCN ice exposed to the hydrogen beam. This shows that the change in morphology in our experiment can be explained by the fact that warm H<sub>2</sub> molecules, which are the dominant species in the hydrogen beam, impinge on the 15 K surface, warm it up locally and change its morphology. This change in morphology could severely limit the yield of our hydrogenation experiments and may explain the low amount of hydrogenation products.

We then proceeded to identify the hydrogenation products. Figure 4 shows that peaks at  $m/z$  30 and 31 are clearly visible in the HCN sample that was hydrogenated for 3 hours, while the unbombarded HCN sample does not have any isotopomer contribution at  $m/z$  30 and 31. This shows that HCN is hydrogenated to methylamine CH<sub>3</sub>NH<sub>2</sub>, because CH<sub>3</sub>NH<sub>2</sub> has its two most characteristic peaks at  $m/z$  30 and 31, as seen in Fig. 2. This also implies that HCN must be first hydrogenated into intermediate species until the CH<sub>3</sub>NH<sub>2</sub> fully saturated species.

Figure 5 shows the  $m/z$  28 and 29 TPD curves without and with hydrogenation for different durations. The  $m/z$  28 curve profile after hydrogen bombardment shows the change in morphology that the HCN sample undergoes. The unexposed HCN sample shows a peak at  $m/z$  29 in the TPD curve, while the exposed HCN sample does not show any excess in the peak at  $m/z$  29 after hydrogenation, which means that no CH<sub>2</sub>NH has been formed. The  $m/z$  29 peak of the unexposed sample can originate

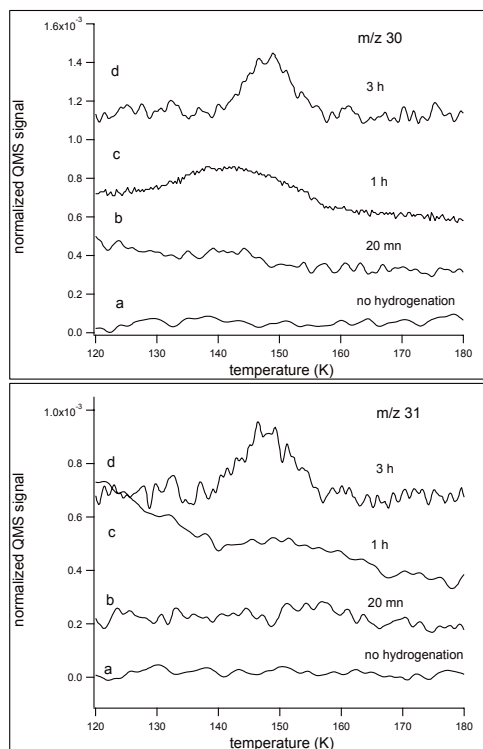


**Fig. 4.** Temperature-programmed desorption curve at  $m/z$  30 and 31 of HCN without exposure to the atomic H beam (a) and after 20 min (b), 1 h (c) and 3 h (d) exposure at 15 K;  $m/z$  30 and 31 evidence the formation of methylamine  $\text{CH}_3\text{NH}_2$  from the hydrogenation of HCN.

from the isotopomers bearing both  $^{13}\text{C}$  and  $^{15}\text{N}$ . However, the abundances of these isotopomers must be very low. Another possible origin for this peak is the  $^{15}\text{N}$ -bearing  $\text{N}_2$  isotopomer, which could originate from the  $\text{N}_2$  deposited along with HCN or from the trapping at 15 K of the chamber residual  $\text{N}_2$ . However, the amount of  $^{15}\text{N}_2$  must be extremely low as well. For the three hour long exposed HCN sample, we know from Fig. 2 that  $\text{CH}_3\text{NH}_2$   $m/z$  29 peak must be approximately in a 1:10 ratio with its  $m/z$  30 most intense peak, which is a very small contribution, in the noise of Fig. 5  $m/z$  29 TPD curve. Figure 2 shows that for  $\text{CH}_2\text{NH}$  the  $m/z$  29 peak is in a 1:2 ratio with the  $m/z$  28 peak, thus an excess on the  $m/z$  29 peak should be clearly visible in Fig. 5 for the 3 h long exposed sample. We have not been able to observe this excess.

Thus we are not able to observe the  $\text{CH}_2\text{NH}$  intermediate HCN hydrogenation product, but we can observe the fully saturated  $\text{CH}_3\text{NH}_2$  hydrogenation product only. Moreover no  $\text{CH}_2\text{NH}$  is present at intermediate exposure durations. After a 20 min hydrogenation neither  $\text{CH}_2\text{NH}$  nor  $\text{CH}_3\text{NH}_2$  are formed. After a 1 h exposure,  $\text{CH}_3\text{NH}_2$  is formed directly and no  $\text{CH}_2\text{NH}$  is detected. This could mean that the cross section for the second hydrogenation step, from methanimine  $\text{CH}_2\text{NH}$  to methylamine  $\text{CH}_3\text{NH}_2$  is much larger than the first hydrogenation step, from HCN to  $\text{CH}_2\text{NH}$ , and that the second hydrogenation reaction is much faster. Both hydrogenation reactions could have an activation barrier and both hydrogenation could occur with trapped H atoms during the TPD experiment at temperature below the HCN thermal desorption. Thus, in both cases, it is difficult to observe the  $\text{CH}_2\text{NH}$  intermediate species.

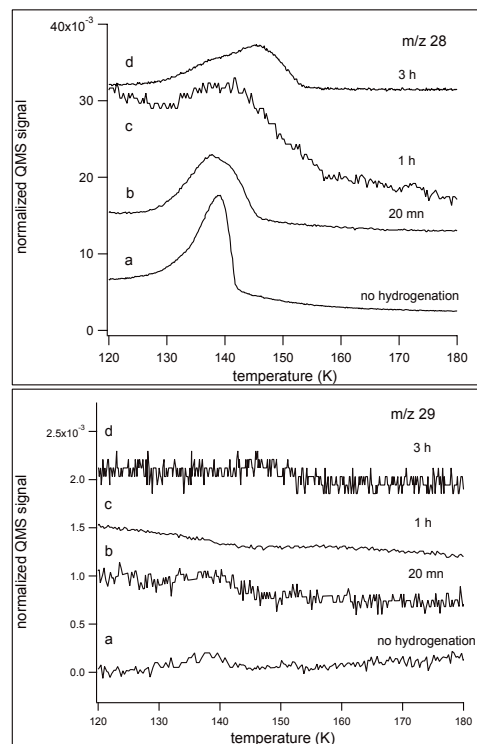


**Fig. 5.** Temperature-programmed desorption spectra of  $m/z$  28 and 29 of HCN without exposure to the atomic H-beam at 15 K (a) and after 20 min (b), one hour (c), and three hours (d) exposure at 15 K;  $m/z$  28 shows the change in morphology of HCN during the hydrogenation experiment. No contribution from  $\text{CH}_2\text{NH}$  is visible in the  $m/z$  29 curve.

### 3.2. Hydrogenation of methanimine $\text{CH}_2\text{NH}$

We want to check independently the  $\text{CH}_2\text{NH}$  to  $\text{CH}_3\text{NH}_2$  second hydrogenation step. To this purpose we hydrogenate pure methanimine  $\text{CH}_2\text{NH}$ .

Gas-phase  $\text{CH}_2\text{NH}$  is condensed at 60 K on the copper surface to eliminate as much as residual  $\text{NH}_3$ . Figure 1 shows the IR spectrum of  $\text{CH}_2\text{NH}$  after deposition. Little  $\text{NH}_3$  is present in our sample. The frozen solid is then exposed during two hours to the atomic hydrogen beam at 15 K. Then the sample is warmed to room temperature during a TPD experiment, with a 5 K/min temperature ramp rate. Figure 6 shows a TPD spectrum of  $\text{CH}_2\text{NH}$  with and without exposure to H atoms.

The hydrogenation experiment was performed twice to check for the reproducibility. The signal was normalized to the total amount of deposited  $\text{CH}_2\text{NH}$ . The two TPD experiments after hydrogenation were compared with a TPD experiment of a  $\text{CH}_2\text{NH}$  witness sample without hydrogenation. The  $m/z$  30 peak shows the hydrogenation of  $\text{CH}_2\text{NH}$  into  $\text{CH}_3\text{NH}_2$ , but the witness sample also exhibits a smaller peak at  $m/z$  30 caused by the  $^{13}\text{CH}_2\text{NH}$  and  $\text{CH}_2^{15}\text{NH}$  isotopomers. The formation of  $\text{CH}_3\text{NH}_2$  is better shown by the peak at  $m/z$  31, where the amount of isotopomers that both have a  $^{13}\text{C}$  and a  $^{15}\text{N}$  is negligible. A TPD experiment of the sample holder exposed to the H-beam during two hours does not show any peak at  $m/z$  30 or  $m/z$  31. Therefore, we can conclude that  $\text{CH}_2\text{NH}$  can be hydrogenated into  $\text{CH}_3\text{NH}_2$ .

We note once again that the exposure to the atomic hydrogen beam has an effect on the physical structure of the  $\text{CH}_2\text{NH}$  solid. If it is not bombarded,  $\text{CH}_2\text{NH}$  desorbs with a typical zeroth-order desorption shape. If bombarded by both H atoms and dominant warm  $\text{H}_2$  molecules, the shape of the  $\text{CH}_2\text{NH}$  desorption

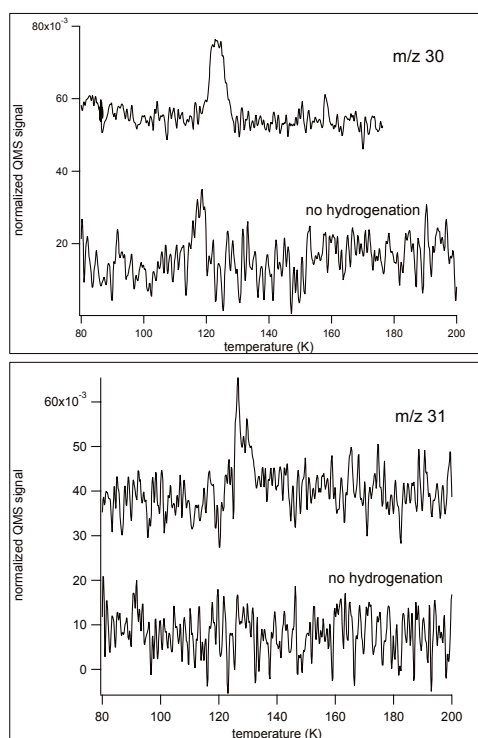


**Fig. 6.** Temperature-programmed desorption spectra of methanimine CH<sub>2</sub>NH after hydrogenation for  $m/z$  30 (top) and  $m/z$  31 (bottom) at  $T = 15$  K. The TPD spectrum of CH<sub>2</sub>NH without hydrogenation is shown in the lower part of the figures for the two masses.

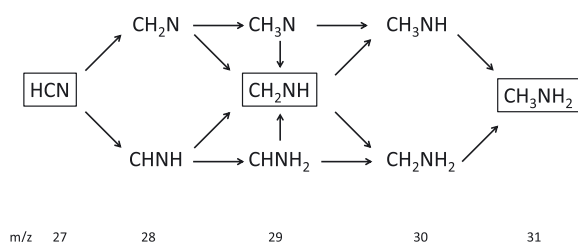


**Fig. 7.** Hydrogenation network of HCN at low temperature. Each arrow represents an hydrogen addition. The stable molecules are into frame. The other molecules are non-stable reaction intermediates.

curve is altered, and the desorption maximum is shifted to higher temperatures by approximately 5 K.

#### 4. Discussion

We have carried out qualitative experiments of hydrogenation of hydrogen cyanide HCN and methanimine CH<sub>2</sub>NH using a hydrogen plasma to generate atomic H, and TPD experiments to detect the hydrogenation products. From these experiments it is possible to draw a chemical reaction network for HCN hydrogenation at low temperature, below its thermal desorption, as shown in Fig. 7. Additional and more quantitative experimental work is needed to evaluate the cross-section of the different hydrogenation processes. However, we show the possibility to hydrogenate a C≡N bond until full saturation in interstellar conditions.

Although hydrogen cyanide HCN (Snyder et al. 1971), methanimine CH<sub>2</sub>NH (Godfrey et al. 1973) and methylamine CH<sub>3</sub>NH<sub>2</sub> (Kaifu et al. 1974; Fourikis et al. 1974) have been detected in the gas phase of the interstellar medium, there is no evidence so far of their presence in its solid-phase, which puts

an upper limit detection to a few tenths of percents of solid H<sub>2</sub>O. Solid-state HCN has been tentatively identified on Triton ices using the AKARI space telescope (Burgdorf et al. 2010) in its 2099 cm<sup>-1</sup> band.

The feasibility of the HCN + H and CH<sub>2</sub>NH + H to form CH<sub>3</sub>NH<sub>2</sub> challenges the grain reaction scenario described in Garrod et al. (2008). The formation of CH<sub>3</sub>NH<sub>2</sub> may be more likely to occur from accreted HCN hydrogenation than from the CH<sub>3</sub> + NH<sub>2</sub> reaction, because the H-atom residence time on the ice surface is significant at 10 K.

Moreover, CH<sub>3</sub>NH<sub>2</sub> is important for the synthesis of amino-acids. It has been shown by Bossa et al. (2009) that the thermal reaction between CH<sub>3</sub>NH<sub>2</sub> and CO<sub>2</sub> leads to the formation of methylammonium methylcarbamate CH<sub>3</sub>NH<sub>3</sub><sup>+</sup>, CH<sub>3</sub>NHCOO<sup>-</sup>, and that the VUV irradiation of this species can give the methylammonium glycinate CH<sub>3</sub>NH<sub>3</sub><sup>+</sup>, NH<sub>2</sub>CH<sub>2</sub>COO<sup>-</sup>, which desorbs giving gas-phase glycine NH<sub>2</sub>CH<sub>2</sub>COOH. In that work CH<sub>3</sub>NH<sub>2</sub> was supposed to be accreted onto the ice surface. Our work shows that CH<sub>3</sub>NH<sub>2</sub> can be formed by direct hydrogenation of accreted HCN, which is a fairly abundant gas-phase species with a typical abundance of a few 10<sup>-9</sup> with respect to H<sub>2</sub>.

Methanimine CH<sub>2</sub>NH is also a possible precursor for glycine. CH<sub>2</sub>NH may react with HCN in an NH<sub>3</sub> environment (Danger et al. 2011) to form aminoacetonitrile NH<sub>2</sub>CH<sub>2</sub>CN, which is considered as a potential glycine precursor through the Strecker reaction in extraterrestrial objects such as meteorites and comets (Bernstein et al. 2002).

The non-observation of the hydrogenation intermediate species in HCN hydrogenation experiments must be discussed in more detail. Following the simple hydrogenation scheme presented in Fig. 7, there are three routes and three hydrogenation intermediate species possible to obtain CH<sub>3</sub>NH<sub>2</sub> from HCN: a nitrene CH<sub>3</sub>NH, a carbene CHNH<sub>2</sub>, and a kinetically more stable species CH<sub>2</sub>NH. Both CH<sub>3</sub>NH and CHNH<sub>2</sub> must easily convert into the stable species CH<sub>2</sub>NH. The non-observation of CH<sub>2</sub>NH can be explained by a larger hydrogenation cross-section for CH<sub>2</sub>NH than for HCN, so the intermediate CH<sub>2</sub>NH is hydrogenated as soon as it is formed. The non-observation of CH<sub>2</sub>NH can be also explained by the fact that the dominant branching ratio of the HCN hydrogenation is towards the nitrene CH<sub>3</sub>NH and the carbene CHNH<sub>2</sub>, and not to CH<sub>2</sub>NH. Because these two species are more reactive, they hydrogenate easily into CH<sub>3</sub>NH<sub>2</sub>. Possibly the CH<sub>3</sub>NH and CHNH<sub>2</sub> species can also react with the dominant species, remaining HCN, to form higher-mass species, like aminoacetonitrile NH<sub>2</sub>CH<sub>2</sub>CN ( $m/z$  56, 55) or N-methylcyanamide CH<sub>3</sub>NHCN. The reaction between intermediate species has been ruled out because we do not observe  $m/z \geq 32$  in our TPD curves. This means that the non-observation of CH<sub>2</sub>NH may be caused by the difference in hydrogenation cross-sections for the two hydrogenation steps.

#### 5. Conclusion

We showed that hydrogen cyanide HCN can be hydrogenated to the fully saturated species methylamine CH<sub>3</sub>NH<sub>2</sub> at low temperature. We propose a possible hydrogenation reaction scheme where methanimine CH<sub>2</sub>NH is a stable intermediate. However, we cannot observe the hydrogenation of HCN into CH<sub>2</sub>NH, whereas we observe the hydrogenation of CH<sub>2</sub>NH into methylamine CH<sub>3</sub>NH<sub>2</sub>. This work shows that it is possible to hydrogenate a C≡N bond in interstellar conditions. Although more quantitative and detailed work needs to be carried out on the HCN hydrogenation scheme, on the relative cross-sections and

efficiencies, the saturation of HCN into CH<sub>3</sub>NH<sub>2</sub> opens interesting perspectives on the formation of amino-acid precursors.

*Acknowledgements.* This work has been funded by the French national programme Physique Chimie du Milieu Interstellaire (PCMI) and the Centre National d'Études Spatiales (CNES). The authors would like to thank Prof. H. Cottin for the HCN synthesis protocol and the referee for the useful comments.

## References

- Accolla, M., Congiu, E., Dulieu, F., et al. 2010, *Phys. Chem. Chem. Phys.*, 13, 8037
- Bernstein, M. P., Dworkin, J. P., Sandford, S. A., Cooper, G. W., & Allamandola, L. J. 2002, *Nature*, 416, 401
- Bisschop, S. E., Fuchs, G. W., van Dishoeck, E. F., & Linnartz, H. 2007, *A&A*, 474, 1061
- Bossa, J. B., Borget, F., Duvernay, F., Theule, P., & Chiavassa, T. 2008, *J. Phys. Chem. A*, 112, 5113
- Bossa, J. B., Duvernay, F., Theule, P., et al. 2009, *A&A*, 506, 601
- Burgdorf, M., Cruikshank, D. P., Dalle Ore, C. M., et al. 2010, *ApJ*, 718, L53
- Danger, G., Bossa, J.-B., de Marcellus, P., et al. 2011, *A&A*, 525, A30
- Dulieu, F., Amiaud, L., Congiu, E., et al. 2010, *A&A*, 511, A30
- Ferris, J. P., & Hagan, W. J. 1984, *Tetrahedron*, 40, 1093
- Fehsenfeld, F. C., Evenson, K. M., & Broida, H. P. 1965, *Rev. Sci. Instrum.*, 36, 294
- Fourikis, N., Tagaki, K., & Morimoto, M. 1974, *ApJ*, 191, 139
- Fuchs, G. W., Cuppen, H. M., Ioppolo, S., et al. 2009, *A&A*, 505, 629
- Garrod, R. T., Weaver, S. L. W., & Herbst, E. 2008, *ApJ*, 682, 283
- Gerakines, P. A., Moore, M. H., & Hudson, R. L. 2004, *Icarus*, 170, 202
- Godfrey, P. D., Brown, R. D., Robinson, B. J., & Sinclair, M. W. 1973, *Astrophys. Lett.*, 13, 119
- Guillemin, J. C., & Denis, J. M. 1988, *Tetrahedron*, 44, 4431
- Hamada, Y., Hashiguchi, K., Tsuboi, M., Koga, Y., & Kondo, S. 1984, *J. Mol. Spec.*, 105, 70
- Hiraoka, K., Ohashi, N., Kihara, Y., et al. 1994, *Chem. Phys. Lett.*, 229, 408
- Hiraoka, K., Miyagoshi, T., Takayama, T., Yamamoto, K., & Kihara, Y. 1998, *ApJ*, 498, 710
- Ioppolo, S., Cuppen, H. M., Romanzin, C., van Dishoeck, E. F., & Linnartz, H. 2008, *ApJ*, 686, 1474
- Ioppolo, S., Cuppen, H. M., van Dishoeck, E. F., & Linnartz, H. 2010, *MNRAS*, 410, 1089
- Jacox, M. E., & Milligan, D. E. 1975, *J. Mol. Spec.*, 56, 333
- Kaifu, N., Morimoto, M., Nagane, K., et al. 1974, *ApJ*, 191, 135
- Matar, E., Congiu, E., Dulieu, F., Momeni, A., & Lemaire, J. L. 2008, *A&A*, 492, L17
- Miyauchi, N., Hidaka, H., Chigai, T., et al. 2008, *Chem. Phys. Lett.*, 456, 27
- Mokrane, H., Chaabouni, H., Accolla, M., et al. 2009, *ApJ*, 705, L195
- Romanzin, C., Ioppolo, S., Cuppen, H. M., van Dishoeck, E. F., & Linnartz, H. 2011, *J. Chem. Phys.*, 134, 084504
- Snyder, L. E., & Buhl, D. 1971, *ApJ*, 163, L47
- Theule, P., Duvernay, F., Ilmane, A., et al. 2011, *A&A*, 530, A96
- Watanabe, N., & Kouchi, A. 2002, *ApJ*, 571, L173